

Simultaneous measurement of surface tension and viscosity using freely decaying oscillations of acoustically levitated droplets

Cite as: Rev. Sci. Instrum. **89**, 015109 (2018); <https://doi.org/10.1063/1.4998796>

Submitted: 03 August 2017 . Accepted: 02 January 2018 . Published Online: 22 January 2018

J. Kremer, A. Kilzer, and M. Petermann 



View Online



Export Citation



CrossMark

ARTICLES YOU MAY BE INTERESTED IN

[TinyLev: A multi-emitter single-axis acoustic levitator](#)

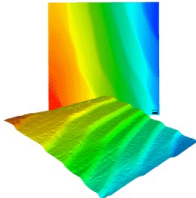
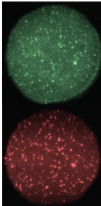
Review of Scientific Instruments **88**, 085105 (2017); <https://doi.org/10.1063/1.4989995>

[Compact acoustic levitation device for studies in fluid dynamics and material science in the laboratory and microgravity](#)

Review of Scientific Instruments **56**, 2059 (1985); <https://doi.org/10.1063/1.1138419>

[A new method for measuring liquid surface tension with acoustic levitation](#)

Review of Scientific Instruments **66**, 3349 (1995); <https://doi.org/10.1063/1.1145506>

 MCL MAD CITY LABS INC. www.madcitylabs.com	<p>Nanopositioning Systems</p> 	<p>Modular Motion Control</p> 	<p>AFM and NSOM Instruments</p> 	<p>Single Molecule Microscopes</p> 
---	--	--	---	--

Simultaneous measurement of surface tension and viscosity using freely decaying oscillations of acoustically levitated droplets

J. Kremer,^{1,a)} A. Kilzer,² and M. Petermann¹

¹Chair of Particle Technology, Ruhr-University Bochum, Universitätsstr. 150, Bochum 44801, Germany

²Chair of Process Technology, Ruhr-University Bochum, Universitätsstr. 150, Bochum 44801, Germany

(Received 3 August 2017; accepted 2 January 2018; published online 22 January 2018)

Oscillations of small liquid drops around a spherical shape have been of great interest to scientists measuring physical properties such as interfacial tension and viscosity, over the last few decades. A powerful tool for contactless positioning is acoustic levitation, which has been used to simultaneously determine the surface tension and viscosity of liquids at ambient pressure. In order to extend this acoustic levitation measurement method to high pressure systems, the method is first evaluated under ambient pressure. To measure surface tension and viscosity using acoustically levitated oscillating drops, an image analysis method has to be developed and factors which may affect measurement, such as sound field or oscillation amplitude, have to be analyzed. In this paper, we describe the simultaneous measurement of surface tension and viscosity using freely decaying shape oscillations of acoustically levitated droplets of different liquids (silicone oils AK 5 and AK 10, squalane, 1-propanol, 1-butanol, 1-pentanol, 1-hexanol, 1-heptanol, and 1-octanol) in air. These liquids vary in viscosity from 2 to about 30 mPa s. An acoustic levitation system, including an optimized standing wave acoustic levitator and a high-speed camera, was used for this study. An image analysis was performed with a self-written Matlab® code. The frequency of oscillation and the damping constant, required for the determination of surface tension and viscosity, respectively, were calculated from the evolution of the equatorial and polar radii. The results and observations are compared to data from the literature in order to analyze the accuracy of surface tension and viscosity determination, as well as the effect of non-spherical drop shape or amplitude of oscillation on measurement. *Published by AIP Publishing.* <https://doi.org/10.1063/1.4998796>

I. INTRODUCTION

Thermophysical properties of liquids are of great importance in many industrial applications. Exact knowledge of these properties is required to ensure a better understanding and design of technical processes. A number of sophisticated measurement methods exist for the determination of surface tension and viscosity under ambient pressure. These measurement methods are commercially available and used but not necessarily the most efficient. Measurement is typically tedious and time-consuming because such methods require contact of the substance of interest with a solid surface. Due to this requirement, the liquid is prone to contamination, an event which must be avoided. The determination of surface tension and viscosity in systems which include gas under high pressure or a supercritical component is even more challenging. Thus, data are rare and not always in agreement. To avoid the aforementioned drawbacks associated with contact to a solid surface, the promising technique of contactless positioning of the liquid using a levitation method should be considered. There are several types of levitation methods, including acoustic, aerodynamic, electrostatic, and magnetic levitation.¹ Acoustic levitation is a powerful tool for the containerless investigation of small solid and liquid material samples. It has been widely investigated as part of studies in the fields of crystallization, evaporation kinetics, monitoring of reactions, heat and mass

transfer, and Raman spectroscopy, to name just a few.² The main advantages of acoustic levitation are that the levitated substance does not need to have specific properties (e.g., ferromagnetism or conductivity), with the sole requirement for a density difference between the sample and the surrounding medium, and that, compared to conventional methods for surface tension and viscosity measurement, only a very small sample volume is needed (1-10 μ l). Due to the lack of interfacial tension and viscosity data for liquids under high pressure, the main goal is to develop a fast measurement method for these properties which can be used under high pressure conditions and which uses acoustic levitation. In order to obtain reliable data under high pressure, the measurement method needs to be tested and validated under ambient pressure first.

Some theoretical and experimental investigations have already been carried out under ambient pressure. They focus on the measurement of surface tension and viscosity of Newtonian liquids with acoustic levitation. Achatz *et al.*³ patented the measurement of surface tension and viscosity using oscillations of acoustically levitated drops in air. Drop shape oscillations are excited by amplitude modulation. Several studies on accuracy of surface tension and viscosity measurements are found in the literature.⁴⁻¹⁴ Trinh, Marston, and Robey⁴ measured the surface tension of some moderately viscous liquids in air. They report the occurrence of at least two resonance peaks in the frequency spectrum of an oscillating drop. Their results on frequency splitting are supported by findings from other investigations, including those by Bayazitoglu and Mitchell⁵

^{a)}kremer@fvt.rub.de

TABLE I. Experimental investigations into surface tension (σ) and viscosity (η) measurements using acoustic levitation under ambient pressure.

Literature	Excitation	Property	Detection	System
Achatz <i>et al.</i> ³	FRF	σ , η	Photodetection system	Liquid drop in air
Trinh, Marston, and Robey ⁴	FRF	σ	Photodetection system	Liquid drop in air
Bayazitoglu and Mitchell ⁵	FRF	σ	Photodetection system	Liquid drop in air
Hosseinzadeh and Holt ⁶	FRF for σ and FD for η	σ , η	Photodetection system	Liquid drop in air
Trinh, Holt, and Thiessen ⁷	FRF, FD	σ	Photodetection system/camera	Liquid drop in air
Trinh, Zwern, and Wang ⁸	FRF for σ and FD for η	σ , η	Photodetection system	Liquid drop in liquid
Biswas, Leung, and Trinh ¹⁰	FRF	σ	Camera	Liquid drop in air
Apfel <i>et al.</i> ¹¹	FD	σ , η	Camera	Liquid drop in air
Trinh and Wang ¹⁴	FRF, FD	σ , η	Photodetection system	Liquid drop in liquid

and, more recently, by Hosseinzadeh and Holt.⁶ Trinh, Holt, and Thiessen⁷ point out that the number of peaks in the frequency spectrum depends on the viscosity of the liquid. For liquids with a viscosity lower than 3 mPa s, three peaks occur, while for liquids with a viscosity higher than 3 mPa s, only two peaks exist.⁷ Trinh, Zwern, and Wang⁸ studied small amplitude oscillations of drops in immiscible liquid systems. They report a higher measured resonance frequency as distortion of the drop increased. Bayazitoglu and Suryanarayana⁹ investigated the effect of static deformation and external forces on the oscillations of levitated droplets in air. They notice frequency splitting due to external forces and note an increase in the measured resonance frequency with greater distortion of the drop.⁹ However, other studies have produced contradictory data. Biswas *et al.*¹⁰ describe a decrease in the resonance frequency with increasing distortion of the drop. Apfel *et al.*¹¹ found that the resonance frequency first increases with increasing aspect ratio up to an aspect ratio of about 1.35, before it decreases again. These particular experimental results were later confirmed by Shi and Apfel¹² using the boundary integral method. Watanabe¹³ conducted a numerical analysis of the shift in the resonance frequency caused by changes in the oscillation amplitude and rotation of the drop. He found a decrease in frequency with increasing amplitude of oscillation. Trinh, Zwern, and Wang⁸ as well as Trinh and Wang¹⁴ investigated to what extent the damping rate of small and large amplitude oscillations is affected by the aspect ratio of acoustically levitated drops in water. They infer a slight trend of increase in the damping constant as the aspect ratio increased. Hosseinzadeh and Holt⁶ state that the inferred viscosity is dependent on the equivalent radius of the drop for large amplitude oscillations (with an amplitude of about 12%) of liquid glycerol-water drops in air. The equivalent radius of the drop is calculated as the radius of a spherical drop with the same volume as the distorted drop.

The use of different techniques to excite shapes into oscillation may cause incongruence between predictions as to what affects measurement. Some authors^{3-10,14} used a steady-state frequency response (FRF) technique to determine surface tension, while others^{7,11,14} used a free decay (FD) method. For the FRF technique, the modulation frequency is increased stepwise and the drop's response is monitored continuously. For the FD method, the drop is initially excited into oscillations, then excitation is ceased and the decaying shape oscillations are recorded. Table I shows a summary of the aforementioned experimental investigations.

For the FRF technique, surface tension is calculated from the frequency occurring at the most prominent peak in the frequency spectrum and viscosity is inferred from the width of the peak. Therefore, the step size during the frequency sweep has to be sufficiently small to accurately determine the frequency of oscillation. Furthermore, the frequency of drop shape oscillation depends on the frequency of amplitude modulation as mentioned by Refs. 3 and 8. The two frequencies only lag in phase and the phase shift depends on the acoustic levitator used. All authors use differently shaped transducers and reflectors, which lead to variations in the sound field. For the FD method, the frequency and damping constant are determined simultaneously from the free decay. As mentioned by Langstaff *et al.*,¹⁵ the drop naturally adapts its eigenfrequency after the cessation of the amplitude modulation. Differences can also be caused by the different techniques used for monitoring of oscillations. Most authors^{3-8,14} use a photodetection system, including a laser and a photodetector, which is focused on the polar radius of the drop or the drop's surface area. Surface tension and viscosity are therefore only calculated from the oscillation of the polar radius or the variation of surface area. Despite the technique used for monitoring of oscillations, no further information is provided regarding differences in the frequency and damping constant using the polar and the equatorial radii. Concluding, we assume that incongruence between the predictions can be caused by the different techniques used for excitation and monitoring of oscillations.

II. MATERIALS AND METHODS

Various alcohols and oils were used in the experiments. All substances were used without further purification. Squalane (purity $\geq 99\%$) was obtained from Sigma Aldrich and the silicone oils AK 5 and AK 10 from Wacker Chemie AG. 1-propanol (purity $\geq 99.5\%$), 1-pentanol (purity $\approx 98\%$), 1-hexanol (purity $\geq 98\%$), 1-heptanol (purity $\geq 99\%$), and 1-octanol (purity $\geq 99\%$) were purchased from Carl Roth, while 1-butanol (purity $\geq 99.5\%$) was obtained from VWR.

A. Experimental procedure

An optimized standing wave acoustic levitation system (Fig. 1) was used for the experiments. The acoustic levitation system consists of an acoustic levitator with equipment for

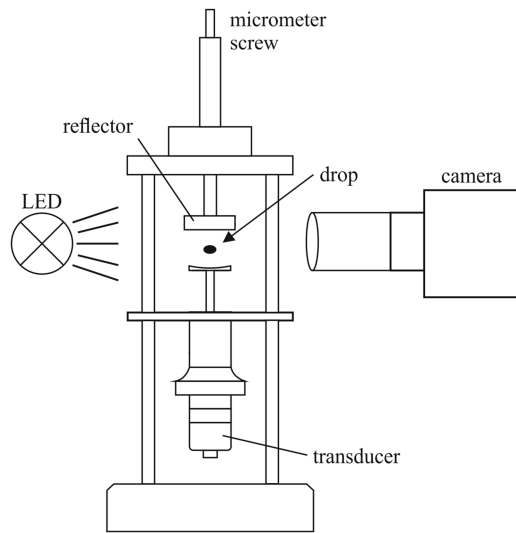


FIG. 1. Acoustic levitation system.

signal generation, a high-speed camera, a light-emitting diode (LED) light source, and a computer for data processing.

The acoustic levitator primarily consists of a piezoelectric transducer and a reflector. Both these parts are curved to enhance the stability of the levitated object. The transducer is driven by a frequency generator (AFG-2112, GW Instek, New-Taipeh, China) and emits ultrasonic waves with a frequency of approximately 41 kHz. The levitation voltage is magnified using an amplifier (33502A, Keysight Technologies, Santa Clara, USA). The ultrasonic waves are reflected by the surface of the reflector. The transducer-reflector distance can be manually adjusted using a micrometer screw to achieve the required resonance conditions. When resonance occurs, a liquid drop is injected into a pressure node of the acoustic standing sound field using a syringe. The acoustic force consists of two forces: the axial force along the axis of levitation (vertical axis), which works against the weight of the drop, and the radial force perpendicular to the axis of levitation. Due to the ratio of these forces ($\approx 5:1$), the levitated drop is ellipsoidal in shape, rather than spherical.²

In order to measure the surface tension and viscosity of an acoustically levitated drop, the drop is excited into oscillations of its shape by a direct amplitude modulation of the transducer drive signal. To do so, the drop was first injected into the sound field. At this point, the amplitude modulation was switched off. After injection, the depth of the amplitude modulation was adjusted to the desired value. The frequency of the amplitude

modulation was swept until the shape oscillation showed a running mode behavior, indicating that the prolate-oblate oscillation was superposed by a rotation. Next, the frequency was reduced until the shape oscillation was at its most prominent, indicating that the axisymmetric fundamental oscillation mode ($l = 2, m = 0$) had been reached. The transition between the running mode behavior and the oscillation in the fundamental mode was observed by eye. For all liquids used, this transition was clearly observable, which was ensured by varying the depth of the amplitude modulation. The amplitude modulation was stopped instantaneously when the desired frequency was reached and the drop exhibited damped harmonic oscillations. To further ensure that the drop exhibited no rotation during measurement, the decay was checked directly after measurement using the high-speed video in slow motion. If there was a rotation, the drop again showed a running mode behavior during the free decay. If the rotation was identified, the measurement was repeated with a lower modulation frequency. During the experiments, the drop is LED backlit and the shape oscillations are monitored using a high-speed camera (CR3000x2, Optronic, Kehl, Germany). The image resolution is 1048×696 pixels and the frame rate is 2000 fps. The high-speed camera is equipped with a macro lens and a tele-converter (EX 2.8/105 DG Macro NAFD OS HSM and TC-2001, Sigma GmbH, Rödermark, Germany). This produces a spatial resolution of 4.7×3.1 mm.

B. Image analysis using Matlab

The high-speed videos were converted into separate images in order to track the evolution of the drop's contours over time. These images were analyzed using a self-written Matlab code. Figure 2(a) depicts a series of high-speed images of an oscillating silicone oil AK 5 drop with a volume of $1.2 \mu\text{l}$ from left to right and top to bottom. The time between two consecutive images is 0.0005 s.

The size of the drop can be determined if the length of one pixel in the high-speed images is known. The pixel length was therefore established using a high precision ruby sphere (Goodfellow, Huntingdon, England) with a known diameter of 2 ± 0.0025 mm. Typically, the length of a recorded high-speed video is 0.5 s and contains 1000 images. The images were saved in a bitmap (BMP) format which provides information about the red-green-blue (RGB) values of every pixel. Each of these images was analyzed using a process which consists of a loop of the following operations. All RGB images were converted into grayscale images. To minimize noise from fluctuations of the light intensity during measurement, a picture

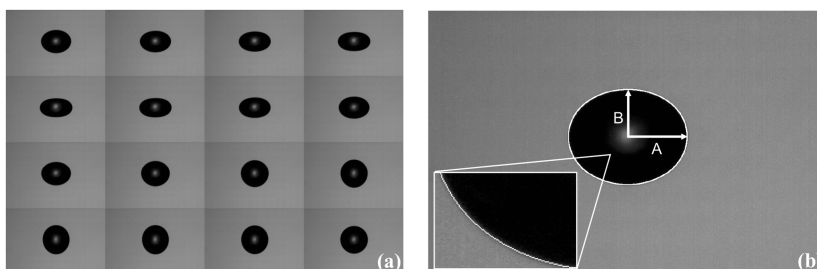


FIG. 2. (a) Original images of the evolution of the shape of an oscillating drop over time and (b) extracted drop contour.

of the background was taken before the measurement and subtracted from every image. The drop contour is extracted using a Canny algorithm which is already available in Matlab. This produces a black and white picture. The drop contour is shown by white pixels, and the background is shown by black pixels. Figure 2(b) depicts the extracted drop contour (white dots), which is plotted onto the original image. In addition, the equatorial (A) and polar (B) radii of the drop are marked. The volume of the drop is determined in the following manner for every image. It is assumed that the drop is symmetrical around the vertical axis. First, the origin of the coordinate system which is used in this experiment is shifted to the center of the drop. The drop was sometimes slightly tilted due to disturbances in the acoustic field. Consequently, a principal axes transformation was performed. Next, the drop contour is divided into two parts: the half to the left and the half to the right of the vertical axis. For every half of the drop contour, the volume is calculated separately by summing up the volumes of cylindrical disks with the equatorial radius and the height of one pixel. The volume of the entire drop is then calculated by taking the average of the volumes of the two results measured for every single image in the video. During one video, the fluctuation in the measured volume is less than 1%. The accuracy of the drop volume calculation was verified using a further high precision ruby sphere with a diameter of 1 ± 0.0025 mm (Goodfellow, Huntingdon, England) and was proven to be greater than 0.5%. The starting point of the damped oscillation is determined using an automated process, which compares the amplitude of the oscillation at every point in time with the previous and following point in time. Finally, the equatorial and the polar radii are monitored over time, from the start of the damped oscillation until the end of the high-speed video.

C. Determination of surface tension and viscosity

The surface tension and viscosity of a liquid can be calculated from the damped harmonic oscillation of a drop by fitting the evolution of the equatorial radius and polar radius (in mm), r_e and r_p , respectively, over time t (in s) according to the following equation:

$$r(t) = r_0 + A \cdot \exp(-\tau t) \cos(2\pi f t). \quad (1)$$

The fitting parameters are the dimensionless amplitude of the drop shape oscillation A , the damping constant τ (in s^{-1}), the frequency f (in Hz), and the equilibrium radius of the drop $r_{e,0}$ or $r_{p,0}$ (in mm). In Fig. 3, a typical result for the polar radius (in mm) over time (in s) of the fitting procedure is shown. For the equatorial radius, the results are comparable regarding the coefficient of determination.

The solid line represents the fit according to Eq. (1) and the dots represent the experimental data points for the polar radius. The precise evolution of the radius over time is described by Eq. (1). The coefficient of determination is higher than 0.8 for the majority of experiments in this paper. It should be noted that the measured oscillation frequency deviates somewhat from the frequency of the amplitude modulation of the standing wave. When the forced amplitude modulation is ceased, the drop almost instantaneously switches to its eigenfrequency.

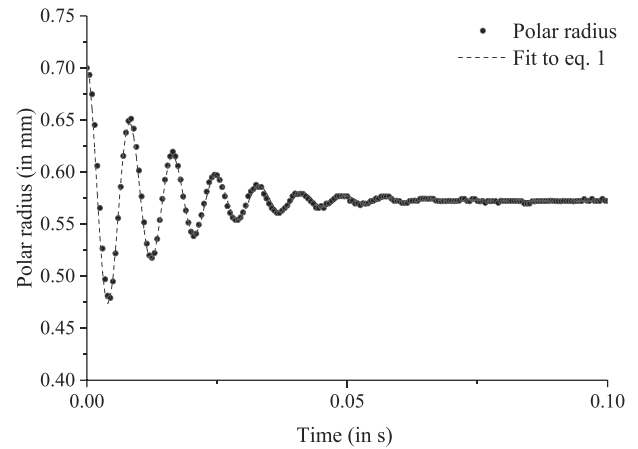


FIG. 3. Evolution of polar radius over time with fit to Eq. (1).

This phenomenon was also observed by Langstaff *et al.*,¹⁵ who used an aerodynamic levitator furnace in their study.

The surface tension of a drop determines the frequency of drop shape oscillation, while the viscosity determines how long it takes for the oscillation to damp out. Rayleigh¹⁶ and Lamb¹⁷ derived the following equations for the oscillations of an inviscid, incompressible drop around a spherical shape. Liquid surface tension σ (in Nm^{-1}) and dynamic viscosity η (in Pa s) are calculated from the liquid density ρ (in $kg\ m^{-3}$), the mode of oscillation l , the volume of the drop V (in m^3), the radius of the volume equal sphere R (in mm), and the oscillation frequency f (in Hz) or the damping constant τ (in s^{-1}). The surface tension σ (in Nm^{-1}) and the viscosity η (in Pa s) can be derived according to the following equations:¹⁶⁻¹⁸

$$\sigma = \frac{3\pi\rho V f^2}{l(l-1)(l+2)}, \quad (2)$$

$$\eta = \frac{\tau\rho R^2}{(l-1)(2l+1)}. \quad (3)$$

The viscosity of the liquid reduces the measured oscillation frequency according to the following expression:¹⁸

$$f = \sqrt{f_{\text{Measurement}}^2 + (2\pi(1/\tau))^{-2}}. \quad (4)$$

Prosperetti¹⁹ pointed out that Eqs. (2) and (3) are only valid for drops with Ohnesorge numbers smaller than 0.1. The Ohnesorge number is given by

$$Oh = \frac{\eta}{\sqrt{\rho\sigma R}}. \quad (5)$$

III. RESULTS AND DISCUSSION

After image analysis, the fitting parameters are saved in an Excel spreadsheet. Table II shows some typical results of image analysis. The experiments were carried out with silicone oil AK 5 at ambient pressure and a temperature of 299.15 K.

The drops in this experiment ranged from 0.8 to 2.7 μl in volume and 0.5 to 0.75 mm in radius. The amplitude of oscillation ranged from 5% to 17% of the drop radius at resting state. It should be noted that the amplitude of oscillations of

TABLE II. Results of image analysis using Matlab [A is the dimensionless amplitude of oscillation, τ is the damping constant in s^{-1} , f is the frequency in Hz, r_0 is the radius of the drop in rest in mm, R^2 is the coefficient of determination of the fit of Eq. (1) to the experimental drop contour, and Oh is the Ohnesorge number of the drop calculated according to Eq. (5)].

No.	Equatorial radius r_e					Polar radius r_p					V (μ l)	R (mm)	Oh
	A_e	τ_e (s^{-1})	f_e (Hz)	$r_{e,0}$ (mm)	R^2_e	A_p	τ_p (s^{-1})	f_p (Hz)	$r_{p,0}$ (mm)	R^2_p			
1	0.05	72.28	146.17	0.60	0.97	0.09	84.53	147.64	0.51	0.97	0.79	0.57	0.05
2	0.07	62.97	113.05	0.73	0.97	0.16	54.64	112.43	0.60	0.96	1.36	0.69	0.05
3	0.09	44.61	81.40	0.93	0.93	0.14	48.30	83.70	0.72	0.96	2.66	0.86	0.04
4	0.08	60.39	117.59	0.71	0.93	0.13	66.84	120.54	0.57	0.96	1.21	0.66	0.05
5	0.10	44.22	85.91	0.89	0.95	0.15	45.38	89.60	0.72	0.99	2.40	0.83	0.04
6	0.10	39.74	95.95	0.83	0.96	0.17	44.68	97.32	0.67	0.99	1.97	0.78	0.04
7	0.07	65.15	117.71	0.72	0.99	0.14	56.32	116.16	0.60	0.98	1.30	0.68	0.05
8	0.07	52.91	106.10	0.76	0.97	0.13	60.61	105.36	0.64	0.94	1.55	0.72	0.04
9	0.07	61.19	119.31	0.71	0.97	0.15	54.11	117.06	0.58	0.92	1.22	0.66	0.05
10	0.07	60.49	132.58	0.66	0.96	0.12	68.21	134.83	0.55	0.99	0.99	0.62	0.05

the polar radius were nearly 1.5–2.5 times higher than those of the equatorial radius. The reason for this difference could be the force ratio in the acoustic field. The coefficient of determination of the fitting procedure according to Eq. (1) was >0.8 for all experiments and the Ohnesorge number was 0.04–0.05. It can therefore be deduced that the utilization of Eqs. (1)–(5) is justified.

A. Measurement of damping constant and frequency

The values for the frequency of oscillation and the damping constant fitted to the equatorial radius differed to those fitted to the polar radius. It was therefore necessary to choose different, appropriate frequency and damping constants for the respective calculations of surface tension and viscosity.

1. Damping constant

The measured damping constants and the resulting dynamic viscosities were compared for all substances. The following options were chosen for the analysis of the damping constant:

- (1) value taken from the equatorial radius τ_e ,
- (2) value taken from the polar radius τ_p ,
- (3) average value of τ_p and τ_e ,
- (4) higher value of τ_p and τ_e ,
- (5) lower value of τ_p and τ_e ,
- (6) value with the larger coefficient of determination.

The liquid's viscosity was calculated using the chosen values for the damping constant and compared to data from the literature.^{20–28} In the case of silicone oils, surface tension and viscosity were measured using conventional methods. The surface tension was analyzed using a tensiometer (DCAT11, Dataphysics, Filderstadt, Germany) and a Wilhelmy plate. The viscosity was determined using a rotational viscometer (Haake Rheostress RS75, Thermo Fisher Scientific, Waltham, USA) equipped with a cylindrical double gap geometry. The absolute deviation, stated in percentages (%), between the values which were measured using acoustic levitation and those which were

obtained from the literature or using conventional methods is calculated according to the following equation:

$$D = \left| \frac{x_{\text{exp}} - x_{\text{lit}}}{x_{\text{lit}}} \right| \times 100. \quad (6)$$

The results are summarized in Table III. All measurements were performed at ambient pressure and a temperature of 298.15 K in the case of alcohols and 299.15 K in the case of oils. All listed values are the average values of at least 30 single drops.

The average absolute deviation from the literature ranged from 2.5% to approximately 15.5%, depending on which analysis method was used. The highest value for the damping constant resulted in the smallest deviation. For simplicity, the highest value damping constant is chosen for the following investigations to determine the dynamic viscosity of the liquid. The reproducibility was calculated as the standard deviation of the mean and was in the range 0.9%–3.2% with the exception of 6.1% in the case of 1-propanol.

2. Frequency

The procedure described in Sec. III A 1 was also used for the determination of surface tension. First, the absolute deviations of the experimental results, which were obtained using analyses (1)–(6), from the literature values were calculated. These deviation results are also shown in Table III. The average absolute deviation from the literature ranged from 4.1% to approximately 7.4%, depending on the type of analysis used. These deviations are much smaller than those found when determining the viscosity. Calculating the resonance frequency from the value measured at the polar radius resulted in the smallest deviation. It should be noted that surface tension calculated from the average of the frequencies measured at the equatorial and the polar radii produced values which were almost as similar to the literature values as those produced using the previous method. Nevertheless, in the following diagrams (Fig. 4), the value taken from the polar radius of the drop was chosen as the measured frequency. The reproducibility was again calculated as the standard deviation of the mean and was in the range of 0.5%–1.0%, with the exception of

TABLE III. Absolute deviation [calculated using Eq. (6)] of the inferred surface tension and viscosity from literature values using analyses (1)–(6). The boldface values highlight the lowest deviation compared to literature.

Substance	Absolute deviation of the viscosity from literature values (%)						Absolute deviation of the surface tension from literature values (%)					
	(1)	(2)	(3)	(4)	(5)	(6)	(1)	(2)	(3)	(4)	(5)	(6)
AK 5	3.37	2.90	3.13	2.84	9.11	0.68	2.87	1.42	2.10	0.22	4.35	0.07
AK 10	12.28	16.07	14.18	1.25	20.87	10.27	5.19	4.86	5.06	2.07	7.70	3.45
Squalane	21.15	26.11	24.69	3.95	45.19	11.60	2.71	0.14	0.48	20.25	15.94	10.22
1-propanol	4.74	7.82	6.28	2.84	15.40	15.15	3.76	4.15	3.93	6.65	1.27	6.65
1-butanol	4.49	1.79	3.14	0.23	6.51	5.93	6.13	7.02	6.57	8.28	4.78	8.28
1-pentanol	5.71	0.53	3.12	2.95	9.20	7.74	5.97	4.71	5.31	7.99	2.68	7.54
1-hexanol	0.65	2.63	1.64	1.09	4.37	1.81	8.70	8.60	8.64	10.44	6.85	10.33
1-heptanol	6.30	9.42	7.86	3.71	12.01	6.25	3.87	2.79	3.32	4.96	1.71	4.91
1-octanol	9.37	11.41	10.39	4.81	15.97	8.07	2.74	2.84	2.83	5.27	0.42	3.83
Average IDI	7.56	8.74	8.27	2.63	15.40	7.50	4.66	4.06	4.25	7.35	5.09	6.14

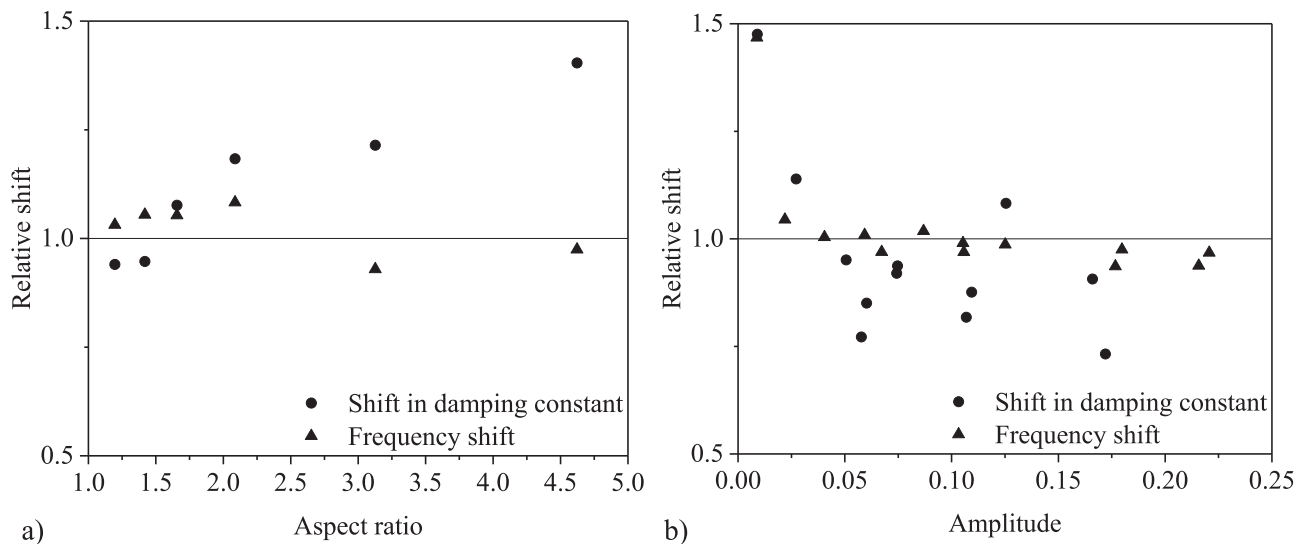


FIG. 4. Frequency shift and shift in the damping constant at varying (a) aspect ratio and (b) amplitude of oscillation.

squalane's 3.8%. It must be pointed out that the deviations using analyses (1)–(6) were much higher for squalane than for any of the other liquids. One reason for this and the higher standard deviation of the mean could be that the Ohnesorge number for squalane drops was approximately 0.2, which exceeds the aforementioned limit of 0.1. Nevertheless, by taking the frequency value from the polar radius and a high value for the damping constant, even for squalane drops, surface tension and viscosity were determined with a comparable accuracy as for the other liquids.

B. Effects on the measurement of damping constant and frequency

As mentioned in the Introduction, it is important to investigate the effect of the acoustic field and the amplitude of oscillation on the measured damping constant and frequency. In order to quantify the effect of the acoustic field, the drop aspect ratio was increased stepwise and the frequency and damping constant were measured alongside this increase. To

adjust the aspect ratio, the voltage which was applied to the acoustic transducer was increased in increments of 1 V until atomization of the drop occurred. All other parameters, such as levitation frequency, the distance between transducer and reflector, and depth of the amplitude modulation, were kept constant. The aspect ratio was calculated as the ratio between the equatorial radius and polar radius of the drop when the oscillation was damped out by viscosity and when the drop was in its resting equilibrium shape [see Fig. 2(b)]. The effect of levitation voltage and amplitude of oscillation on the determination of the damping constant was analyzed using squalane. As mentioned before, there are some predictions on the shift in the frequency and damping constant due to the oscillation amplitude, which can be found in the literature. The level of dependence of the amplitude of oscillation on the damping constant was analyzed using silicone oil AK 5 drops. In order to adjust the amplitude of oscillation, the depth of the amplitude modulation was increased, while the levitation voltage, frequency, and distance between the transducer and the reflector were kept constant. The shift in the

damping constant and frequency was calculated as the ratio between the following two values. The first value was the measured value for the damping constant or the frequency which was corrected using Eq. (4). The second value was the corresponding damping constant or frequency value derived from literature values for surface tension and viscosity using Eqs. (2) and (3), respectively. The experimental points again represent the average value of ten different drops. The results are shown in Fig. 4. The triangles represent the observed frequency shift and the circles represent the shift in the damping constant.

The effect of aspect ratio on the shift in the frequency and damping constant is shown in Fig. 4(a). The frequency shift first increases with increasing aspect ratio, then the frequency decreases with further increasing aspect ratio. This dependency is also reported by Apfel *et al.*,¹¹ who observed this phenomenon in experiments, and Shi and Apfel,¹² who derived it from numerical simulations. For an aspect ratio between 1.1 and 1.2, the maximum observed frequency shift is approximately 2%.^{11,12} In this study, the frequency shift for an aspect ratio of 1.2 is 3%. It is not possible to reduce the aspect ratio to less than 1.1 using the acoustic levitation system. The maximum observed frequency shift in this experiment is approximately 8% at an aspect ratio of 2.1, which is higher than the frequency shift observed and obtained by Apfel *et al.*¹¹ and Shi and Apfel.¹² The reason for this may be the fact that changing the aspect ratio is not possible without changing the amplitude of oscillation at the same time. The deviation of the measured damping constant from the theoretical value calculated using Eq. (3) increases as the aspect ratio is increased. This observation is in line with the results from Trinh and Wang's study.¹⁴ For aspect ratios of less than 1.5, the shift in the damping constant is approximately 5%–6%. This results in the same magnitude of change in viscosity due to the one-to-one relationship between the damping constant and the inferred dynamic viscosity. For an aspect ratio as large as 4.6, the shift in the damping constant is nearly 40%.

Figure 4(b) depicts the dependency of the shift in the frequency and damping constant on the oscillation amplitude. For oscillation amplitudes of less than 2%, the pixel-based image analysis fails because the change in radius is smaller than, or very close to, the detection limit. Therefore, the shift in the frequency and damping constant reaches up to 50%. It was possible to observe a decrease in the frequency shift with increasing amplitude of oscillation. The same trend was predicted by Watanabe¹³ in a numerical simulation. For oscillation amplitudes higher than 17% of the drop radius at rest, the observed shift in frequency is approximately 3%–7%. For amplitudes between 5% and 15%, the shift in the frequency is only approximately 2%–3%, resulting in a maximum error of 6% in surface tension measurement. The amount by which frequency is shifted in this investigation is again higher than that derived by Watanabe.¹³

For amplitudes between 5% and 13%, the values for the shift in the damping constant are scattered and no significant trend is observed. For oscillation amplitudes higher than 13% of the drop radius at rest, a slight decreasing tendency can be observed. This investigation did not reveal a dependence of the

inferred viscosity on the drop equivalent radius as reported by Hosseinzadeh and Holt,⁶ even though oscillations with amplitudes of about 5%–15% were analyzed. Hosseinzadeh and Holt⁶ report an increase in inferred viscosity for equivalent drop radii larger than 1.15 mm. The equivalent drop radii for all drops in this investigation are smaller than 1 mm.

In conclusion of the results presented above, it can be inferred that the levitation voltage should be adjusted to as low a level as possible to avoid shifts in the damping constant and frequency due to the aspect ratio. Furthermore, the amplitude of oscillation should be kept between 5% and 15% to avoid errors due to noise in the image analysis and large amplitude effects.

C. Limitations of the proposed measurement method

In order to simultaneously measure surface tension and viscosity from the freely decaying oscillations, it was important to ensure that the drop acts as a damped harmonic oscillator. Depending on the drop radius and the liquid properties, two relaxation regimes are possible in the case of the freely decaying small amplitude oscillations of a spherical liquid drop. The shape relaxation is either an aperiodic or a damped oscillation. The drop recovers its equilibrium shape exponentially or exhibits damped oscillations described by a damping constant.²⁹

Given the stability of the levitated drop and the pixel-based image analysis, it is best to use drops with volumes of between 0.5 and 5 μl in the acoustic levitation system. This results in drop equivalent radii of 0.5–1.1 mm. Assuming a liquid with a density of 900 kg/m^3 and a surface tension of 25 mN/m , the limit in viscosity measurement of the proposed method can be calculated according to the following equation:²⁹

$$\eta_{crit} = \sqrt{R\sigma\rho}. \quad (7)$$

This produces critical viscosity values of 106 mPa s for 0.5 μl and 335 mPa s for 5 μl drops. For liquids with a viscosity lower than the critical value, the relaxation will be a damped oscillation according to Eq. (3). For viscosities higher than the critical value, the relaxation will be aperiodic. Even though there are some approaches^{30,31} for non-Newtonian liquids, the proposed method is limited to Newtonian fluids because the shear rate in the drop is not known and not constant. Based on own experimental investigations, the shear rate can be estimated to be very high (about 10 000–15 000 s^{-1}).

IV. CONCLUSIONS

In this paper, we describe the measurement of surface tension and viscosity of liquids using an acoustic levitation system. Surface tension and viscosity of various alcohols and oils with viscosities between 2 and 30 mPa s were simultaneously measured by analyzing freely decaying oscillations. The acoustically levitated drop was initially excited into axisymmetric, oblate-prolate shape oscillations through amplitude modulation. When the amplitude modulation was ceased, the drop exhibited damped oscillations. The frequency of oscillation is affected by surface tension and the time until oscillations are damped out by the viscosity of the liquid. The damping

constant and frequency were measured at the equatorial and polar radii of the drop. The values differed somewhat from one another. Consequently, different options for determining the damping constant and frequency were discussed, taking into account the accuracy of the measurement.

Accurate measurements of viscosity with a maximum absolute error of 5% are possible when the higher value of the damping constant is used. The maximum error in surface tension determination is higher (9%). The frequency of oscillation was measured using the polar radius of the drop. Predictions of shifts in the frequency and damping constant and how these affect inferred surface tension and viscosity were found in the literature. In this literature, the effect of aspect ratio and amplitude of oscillation on measurement were investigated. The experimental results indicate that both the aspect ratio and amplitude of oscillation affect the inferred viscosity and surface tension. With increasing aspect ratio, the measured frequency first increases and then decreases. The maximum observed shift is 8% for an aspect ratio of 2.1, which results in a shift in inferred surface tension of 17.6%. The shift in the damping constant increases with increasing aspect ratio. The shift is smaller than 6% for aspect ratios below 1.5 and results in the same magnitude of change in viscosity. The values for the shift in the damping constant due to the amplitude of oscillation were scattered but a slight decreasing trend with increasing amplitude of oscillation can be found. The aspect ratio should therefore be kept as low as possible and the amplitude of oscillation should be in the range of 5%–15%.

For the proposed measurement method, no tedious calibration of the experimental system is required. Only a reference image of a ruby sphere has to be taken to determine the pixel length in a high-speed image. Therefore, the measurement is faster than conventional methods for the determination of surface tension and viscosity. Using conventional methods such as a tensiometer or a rotational viscometer, normally measurement is carried out in triplets and the apparatus has to be cleaned afterwards. This takes about 15 min for surface tension measurement and the same amount of time for viscosity measurement. To measure surface tension and viscosity with acoustic levitation of three different drops, 6 min of measurement time followed by 9 min of image analysis are needed. Therefore we assume that the measurement time is reduced by half. Further research is planned on the measurement of interfacial tension and viscosity under high pressure using the

described measurement method. Interfacial tension and viscosity of liquids in contact with carbon dioxide under high pressure will then be measured under a range of conditions, from the gaseous to the supercritical state of carbon dioxide.

- ¹V. Vandaele, P. Lambert, and A. Delchambre, *Precis. Eng.* **29**, 491 (2005).
- ²E. G. Lierke, *Acustica* **82**, 220 (1996).
- ³M. Achatz, W. Heide, E. G. Lierke, G. H. Seger, German patent 2709698 A1 (9 July 1978).
- ⁴E. H. Trinh, P. L. Marston, and J. L. Robey, *J. Colloid Interface Sci.* **124**(1), 95 (1987).
- ⁵Y. Bayazitoglu and G. F. Mitchell, *J. Thermophys. Heat Transfer* **9**(4), 694 (1995).
- ⁶V. A. Hosseinzadeh and R. G. Holt, *J. Appl. Phys.* **121**, 174502 (2017).
- ⁷E. H. Trinh, R. G. Holt, and D. B. Thiessen, *Phys. Fluids* **8**(1), 43 (1996).
- ⁸E. H. Trinh, A. Zwern, and T. G. Wang, *J. Fluid Mech.* **115**, 453 (1982).
- ⁹P. V. R. Suryanarayana and Y. Bayazitoglu, *Phys. Fluids A* **3**(5), 967 (1991).
- ¹⁰A. Biswas, E. W. Leung, and E. H. Trinh, *J. Acoust. Soc. Am.* **90**(3), 1502 (1991).
- ¹¹R. E. Apfel, R. G. Holt, Y. Tian, T. Shi, and X. Zheng, in *Joint Launch + One Year Science Review for USML-1 and USMP-1 With the Microgravity Measurement Group, Huntsville, USA, 22–24 September, 1993* (N. Ramachandran, 1993), p. 339.
- ¹²T. Shi and R. E. Apfel, *Phys. Fluids* **7**(7), 1545 (1995).
- ¹³T. Watanabe, in *ECCOMAS CFD 2006: Proceedings of the European Conference on Computational Fluid Dynamics*, edited by P. Wesseling, E. Onate, and J. Périaux, Egmond aan Zee, The Netherlands, 2006.
- ¹⁴E. H. Trinh and T. G. Wang, *J. Fluid Mech.* **122**, 315 (1982).
- ¹⁵D. Langstaff, M. Gunn, G. N. Greaves, A. Marsing, and F. Kargl, *Rev. Sci. Instrum.* **84**, 124901 (2013).
- ¹⁶Lord Rayleigh, *Proc. R. Soc. Lond.* **29**, 71 (1879).
- ¹⁷H. Lamb, *Hydrodynamics*, 6th ed. (Cambridge University Press, Cambridge, 1932), p. 475.
- ¹⁸E. Becker, W. J. Hiller, and T. A. Kowalewski, *J. Fluid Mech.* **231**, 189 (1991).
- ¹⁹A. Prosperetti, *J. Fluid Mech.* **100**(2), 333 (1980).
- ²⁰J. L. Trenzado, E. Romano, L. Segade, M. Nieves Caro, E. González, and S. Galván, *J. Chem. Eng. Data* **56**, 2841 (2011).
- ²¹S. Azizian and N. Bashavard, *J. Chem. Eng. Data* **50**, 1303 (2005).
- ²²R. Sadeghi and S. Azizpour, *J. Chem. Eng. Data* **56**, 240 (2011).
- ²³L. Segade, J. Jiménez de Llano, M. Domínguez-Pérez, Ó. Cabeza, M. Cabanas, and E. Jiménez, *J. Chem. Eng. Data* **48**, 1251 (2003).
- ²⁴V. Mutalik, L. S. Manjeshwar, M. Sairam, and T. M. Aminabhavi, *J. Mol. Liq.* **129**, 147 (2006).
- ²⁵A. S. Al-Jimaz, J. A. Al-Kandary, and A.-H. M. Abdul-Latif, *Fluid Phase Equilib.* **218**, 247 (2004).
- ²⁶Z. Shan and A.-F. A. Asfour, *J. Chem. Eng. Data* **44**, 118 (1999).
- ²⁷A. Bhattacharjee and M. N. Roy, *J. Chem. Eng. Data* **55**, 5914 (2010).
- ²⁸M.-J. Lee, T.-K. Lin, Y.-H. Pai, and K.-S. Lin, *J. Chem. Eng. Data* **42**, 854 (1997).
- ²⁹P.-H. Haumesser, J. Bancillon, M. Daniel, M. Perez, and J.-P. Garandet, *Rev. Sci. Instrum.* **73**(9), 3275 (2002).
- ³⁰G. Brenn and S. Teichtmeister, *J. Fluid Mech.* **733**, 504 (2013).
- ³¹G. Brenn and G. Plohl, *J. Non-Newtonian Fluid Mech.* **223**, 88 (2015).